Molecular Therapy
Nucleic Acids
Original Article

lncRNA RMST Suppressed GBM Cell Mitophagy through Enhancing FUS SUMOylation

Changhong Liu,[1,2] Zixuan Peng,[1,3] Peiyao Li,[1,3] Haijuan Fu,[1,3] Jianbo Feng,[1,3] Yan Zhang,[1,3] Tao Liu,[1,3] Yang Liu,[1,3] Qing Liu,[4] Qiang Liu,[5] Di Li,[1,3] and Minghua Wu[1,3]

[1]Hunan Provincial Tumor Hospital and the Affiliated Tumor Hospital of Xiangya Medical School, Central South University, Changsha, Hunan 410013, China; [2]Institute of Medical Sciences, The Second Hospital of Shandong University, Jinan, Shandong 250033, China; [3]The Key Laboratory of Carcinogenesis of the Chinese Ministry of Health, The Key Laboratory of Carcinogenesis and Cancer Invasion of the Chinese Ministry of Education, Cancer Research Institute, Central South University, Changsha, Hunan 410008, China; [4]The Xiangya Hospital, Central South University, Changsha, Hunan 410008, China; [5]The Third Xiangya Hospital, Central South University, Changsha, Hunan 410011, China

Long non-coding RNAs (lncRNAs) play a significant role in post-translational modifications of proteins, yet the importance of lncRNAs for SUMOylation is unknown. rhabdomyosarcoma 2 associated transcript (RMST) expression in glioma tissues and normal brain tissues was measured by quantitative real-time PCR and *in situ* hybridization. The functional roles of RMST in astrocytomas were demonstrated by a series of *in vitro* experiments. The potential mechanisms of RMST for SUMOylation were investigated by RNA immunoprecipitation, RNA pull-down, western blotting, and coimmunoprecipitation assays. We first demonstrated the oncogenic activity of lncRNA RMST by inhibiting glioma cells mitophagy. We also first determined that RMST is an enhancer of FUS SUMOylation, especially boosting SUMO1 modification at K333. SUMOylation induced by RMST contributes to the interaction between FUS and heterogeneous nuclear ribonucleoprotein D (hnRNPD) and stabilized their expression and cells mitophagy. Importantly, lncRNA RMST could serve as a promising prognostic factor for glioma patients. Our results demonstrated a previously unknown function of lncRNAs worked as an enhancer in FUS SUMOylation, and RMST will be a significant guide for the development of medications targeting gliomas.

INTRODUCTION

Posttranslational modification of proteins has proven to be a critical regulatory mechanism to control protein function, including phosphorylation, ubiquitination, small ubiquitin-related modifier (SUMO), acetylation, et al.[1] SUMO is a kind of reversible and highly dynamic post-translational modification of protein,[2] and it is known to be important for mRNA processing, genome stability, nucleocytoplasmic transport, and cell growth regulation.[3,4] SUMO1, -2, -3, and -4 are identified as SUMO modifiers; the four SUMO proteins had distinct functions in SUMOylation, including differences in subcellular localization, responses to environmental conditions, and susceptibilities to various SUMO proteases.[5,6] SUMO1 used ATP hydrolysis to covalently link SUMO to its active site cysteine and subsequently transfer SUMO to the active site on SUMO2. With the help of SUMO3, the SUMO2 further transfers SUMO onto substrates.[7] More proteins have been found to be modified by SUMO1 that include transcription factors, nuclear receptors, and transcriptional cofactors.[8] Although a large body of knowledge had been accumulated about the biological functions of SUMO, the mechanisms by which SUMO is mediated are largely unknown.

Recently, the roles of long non-coding RNAs (lncRNAs) have attracted considerable attention. Integrative genomic studies have revealed tens of thousands of lncRNA in the human genome.[9] Many of them are uniquely expressed in tissues and aberrantly expressed in specific cancer.[10] lncRNAs played a significant role in oncogenic or tumor-suppressive pathways and have similar diagnostic and prognostic power to that of mRNA and microRNA (miRNA) signatures.[11] Many lncRNAs contributed to post-translational modifications of proteins,[12] such as phosphorylation, acetylation, and glycosylation, that regulate protein degradation or production.[13,14] lncRNA NKILA inhibited nuclear factor κB (NF-κB) signaling by masking the phosphorylation sites of IκB;[15] lncRNA HOTAIR upregulated androgen receptor expression by inhibiting ubiquitination of the androgen receptor;[16] lncRNA-p21 upregulated hypoxia inducible factor 1 subunit alpha (HIF-1α) expression by inhibiting ubiquitination of HIF-1α.[17] lncRNA MALAT1 regulates the acetylation of p53 through MALAT1 interacting with DBC1.[18] However, whether lncRNA plays a role in SUMOylation is not clear yet.

In our previous studies, we found lncRNAs CASC2c, LINC00470, CRNDE, RMST, CRYM-AS1, and PRKAG2-AS1 had different expression between astrocytoma and normal brain tissues, and we further confirmed their specific roles in glioma.[19] CASC2c regulated CPEB1 expression through functioning as a competing endogenous RNA to compete for binding miR-101;[19] one side, CPEB1 as a new target of miR-101, it was regulated directly by the tumor suppressor miR-101,

Received 15 February 2019; accepted 6 January 2020;
https://doi.org/10.1016/j.omtn.2020.01.008.

Correspondence: Minghua Wu, The Key Laboratory of Carcinogenesis of the Chinese Ministry of Health, The Key Laboratory of Carcinogenesis and Cancer Invasion of the Chinese Ministry of Education, Cancer Research Institute, Central South University, Changsha, Hunan 410013, China.
E-mail: wuminghua554@aliyun.com

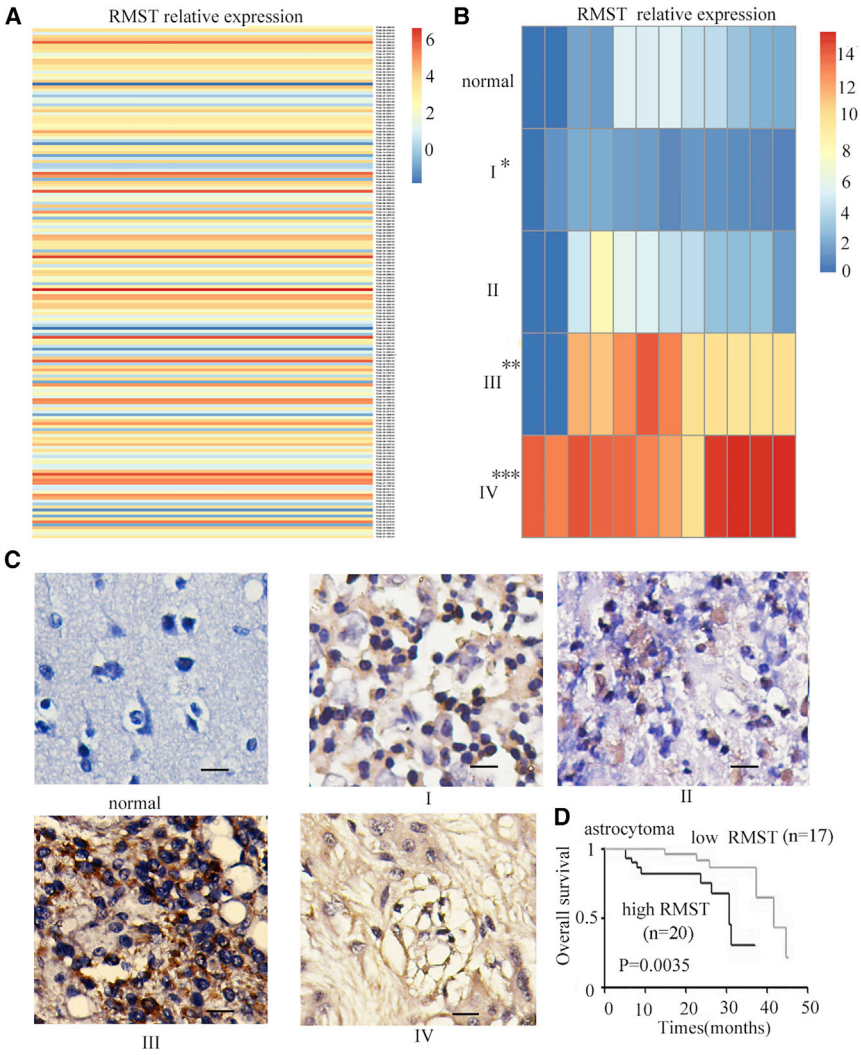

Figure 1. RMST Was Correlated with Malignant Progression of Astrocytoma

(A) Heatmap of RMST expression levels in normal brain tissues and astrocytoma from the TCGA dataset. (B) Heatmap of quantitative real-time PCR analysis of RMST expression levels with different World Health Organization (WHO) grades of astrocytoma (*$p < 0.05$, **$p < 0.01$). (C) The expression levels of RMST were detected in astrocytoma tissues via *in situ* hybridization. Scale bars, 10 μm. (D) Kaplan-Meier analysis of 37 astrocytoma patients with high RMST expression versus low RMST expression (23 astrocytoma patients' data were censored at the last follow-up).

and miR-101 downregulated the expression of CPEB1 through reversing the methylation status of the CPEB1 promoter by regulating the presence on the promoter of the methylation-related histones H3K4me2, H3K27me3, H3K9me3, and H4K20me3.[20] CASC2c interacted with miR-338-3p to inhibit F10 expression and secretion and repressed M2 subtype macrophage polarization in glioma, but it did not function as a competing endogenous RNA to sponge miR-338-3p.[21] LINC00470 not only served as an AKT activator to promote glioblastoma (GBM) progression,[22] but it also could coordinate the epigenetic regulation of ELFN2 to inhibit glioma cell autophagy.[23] RMST (rhabdomyosarcoma 2-associated transcript) is a lncRNA, located in chromosome band 12q23.1.[24] Currently, the function of RMST is mainly reported in breast cancer, and RMST plays a role of tumor suppressor in triple-negative breast cancer through inhibiting cell proliferation, invasion, and migration.[25,26] Other studies showed that RMST also plays a critical role in neuronal differentiation and brain development.[27,28] To date, there are not known reports about the expression and functions of RMST in glioma.

Here, we first detected a higher expression of RMST, which is a better prognosis marker. We also first found that RMST promoted glioma cell proliferation by inhibiting cells' mitophagy. In addition, RMST could bind with FUS (fused in sarcoma) and promote FUS SUMOylation to promote the degradation of ATG4D.

RESULTS

Higher RMST Expression Was Accompanied by Worse Prognosis for Glioma Patients

To address the role of RMST in glioma, we first compared RMST expression between glioma tissues and normal brain tissues based on the TCGA database; RMST expression was higher in glioma tissues than in normal brain tissues (Figure 1A). To support the finding, we analyzed the expression of RMST in clinical specimens of astrocytoma patients by quantitative real-time PCR and found that RMST levels significantly increased in GBM tissues (Figure 1B). We further performed *in situ* hybridization to verify the different degrees of expression level of RMST in astrocytoma tissues. Of the 60 specimens, 45 cases of astrocytoma presented higher (score ≥ 3) and 15 cases showed lower (score <3) RMST expressions, and the positive expression of RMST was mainly located in cytoplasm (Figure 1C).

Then, we assessed the relationship of RMST expression and astrocytoma patient survival by Kaplan-Meier survival. Patients with higher RMST expression (>median level = 4.57) have a worse prognosis (Figure 1D). Then, we evaluated the clinical relevance for astrocytoma patients and found that expression of RMST was correlated histological grade, 95.6% (43/45) high-grade glioma (HGG) with higher RMST expression (Table 1).

RMST Functions as a Potential Oncogenic lncRNA to Suppress GBM Cell Mitophagy

To further demonstrate the roles of RMST in astrocytoma, we first analyzed RMST expression in GBM cell lines by quantitative

Table 1. Correlation between the Clinicopathological Factors and Expression of RMST in Astrocytoma

	RMST			
Variable		low	high	*P*
Total(N=60)	N	15	45	
Sex				
Male	16	4(26.6%)	12(26.7%)	
Female	44	11(73.4%)	33(73.3%)	0.36
Age				
≤42	22	6(40.0%)	16(35.6%)	
>42	38	9(60.0%)	29(64.4%)	0.47
Grade				
LGG(I+II)	20	8(53.3%)	2(4.4%)	
HGG(III+IV)	40	7(46.6%)	43(95.6%)	0.04

real-time PCR. RMST was expressed higher in U251 and expressed lower in U87, relatively (Figure 2A). We knocked down RMST by designing three small interfering RNAs (siRNAs) targeting sequences and screened si-RMST-1, which effectively silenced endogenous RMST expression in U251 cells (Figure 2B); as well, we overexpressed RMST in U87 cells (Figure 2C). RMST knockdown resulted in a decrease of U251 cell proliferation by cell counting kit-8 (CCK-8) and EdU assay (Figures 2D and 2E) and inhibited U251 cell migration and invasion (Figures 2F). Overexpression of RMST promoted the proliferation, migration, and invasion of U87 cells (Figures 2D, 2E, and 2G). Moreover, silencing RMST increased LC3II expression, and transmission electron microscopy results showed that there were more autophagic vacuoles in U251 cells after knockdown of RMST (Figures 2H and 2I); RMST overexpression inhibited the levels of LC3II. Further, the expression of PINK1, Beclin-1, ATG5, and ATG4D, which are markers of mitophagy, were also increased or reduced in GBM cells after knockdown or overexpression RMST (Figures 2H); these results suggested that RMST was involved in mitophagy of GBM cells. Next, we performed immunofluorescence staining and found the colocalization between RMST and apoptosis inducing factor (AIF) (AIF was a marker of mitochondria) in mitochondria of U251 cells (Figures 2J). To further confirm the finding, we also detected the effects of RMST on GBM cell mitophagy through mitophagy detection kit; the results showed that RMST knockdown increased fluorescent intensity in U251 cells, suggesting mitochondria produce more autophagosomes (Figures 2K); that is, RMST inhibited GBM cell mitophagy. These results confirmed the oncogenic activity of RMST by inhibiting cell mitophagy.

RMST Interacted with FUS and SUMOylated FUS at K333

To demonstrate the mechanism of RMST in GBM cell mitophagy, the mirlncRNA website was used to find that RMST may interact with FUS. Then, we performed an RNA immunoprecipitation assay, in which the RMST-FUS complex was immunoprecipitated using FUS antibody. Compared with the immunoglobulin G (IgG)-bound sample, the FUS had a significant increase in the amount of RMST (Figures 3A). Further, different lengths of RMST mutations were constructed then an RMST RNA pull-down assay with FUS antibody was performed. We found that 1740-2101bp of RMST was important for the binding between RMST and FUS (Figure 3B).

Subsequently, we asked whether and how RMST regulated GBM cell autophagy through FUS. SUMOylation is now recognized as a regulatory process involved in mitosis,[6] meiosis,[6] differentiation and development,[6] and senescence,[6] but there are no reports about whether SUMOylation was involved in cell autophagy regulation. Hence, SUMOplotTM Analysis Program (http://www.abcepta.com/sumoplot) and SUMOsp 2.0 software (http://sumosp.biocuckoo.org/online.php) were used to predict and find the possible SUMOylation sites of FUS, where there is one consensus motif in RRM domain of FUS (Figure 3C). Ubc9 is a monomeric E2-conjugating enzyme that transfers SUMO to the substrate protein, where SUMO is covalently linked to a lysine residue through an isopeptide bond between the epsilon amino group of the lysine and the carboxyl group of the C-terminal glycine on SUMO.[8] As shown in Figure 3D, we have confirmed that FUS interacted with Ubc9 in U251 cells, which implies that FUS could be SUMOylated in GBM cells. Interestingly, our results indicate that FUS was strongly modified by SUMO1 and SUMO2 but very weakly modified by SUMO3 in U251 cells (Figure 3E); however, RMST enhanced the SUMOylation modification of SUMO1 and SUMO2 on FUS, especially in SUMO1. Thus, we focused on the effect of RMST on potential modification of SUMO1 for FUS. We found that SUMO1 modification of FUS was weakened after RMST knockdown (Figure 3F). SENP1 is an important deSUMOylation enzyme for SUMO1-conjugated substrates; we also found that levels of SUMOylation FUS could be easily observed after SENP1 knockdown (Figure 3G). The above results suggested that RMST could boost the FUS SUMOylation modification by SUMO1 and may function as a SUMO1 modification enzyme.

To determine SUMOylation sites in FUS by SUMOsp 2.0 software and UMOplotTM analysis, we predicted that the score was the highest on FUS SUMOylation motifs at residue K333 (Table 2). We constructed plasmids expressing wild-type or mutant FUS, in which the predicted Lys (K) was replaced by Arg (R) to block SUMOylation. Then, SUMOylation assays were performed in HEK293 cells (Figure 3H) and U251 cells (Figure 3F) by cotransfecting mutant K333R, with or without HA-SUMO1, with wild-type FUS. As expected, K333 was indeed a key SUMOylation site of FUS (Figures 3F and 3H).

SUMOylation by RMST Maintained FUS Stability via Inhibiting Its Ubiquitination

Next, we wondered whether SUMO1 modification of FUS by RMST affects its protein stability. First, we showed that the protein expression level of FUS was significantly increased in the deSUMOylation enzyme SUMO specific peptidase 1 (SENP1)-knockdown HEK293 cells (Figure 4A). Meanwhile, we also found that the protein expression level of FUS in the SENP1-knockdown GBM cells was much higher than that in control cells (Figure 4A). These data implied that SUMO1 modification potentially stabilizes FUS protein. To

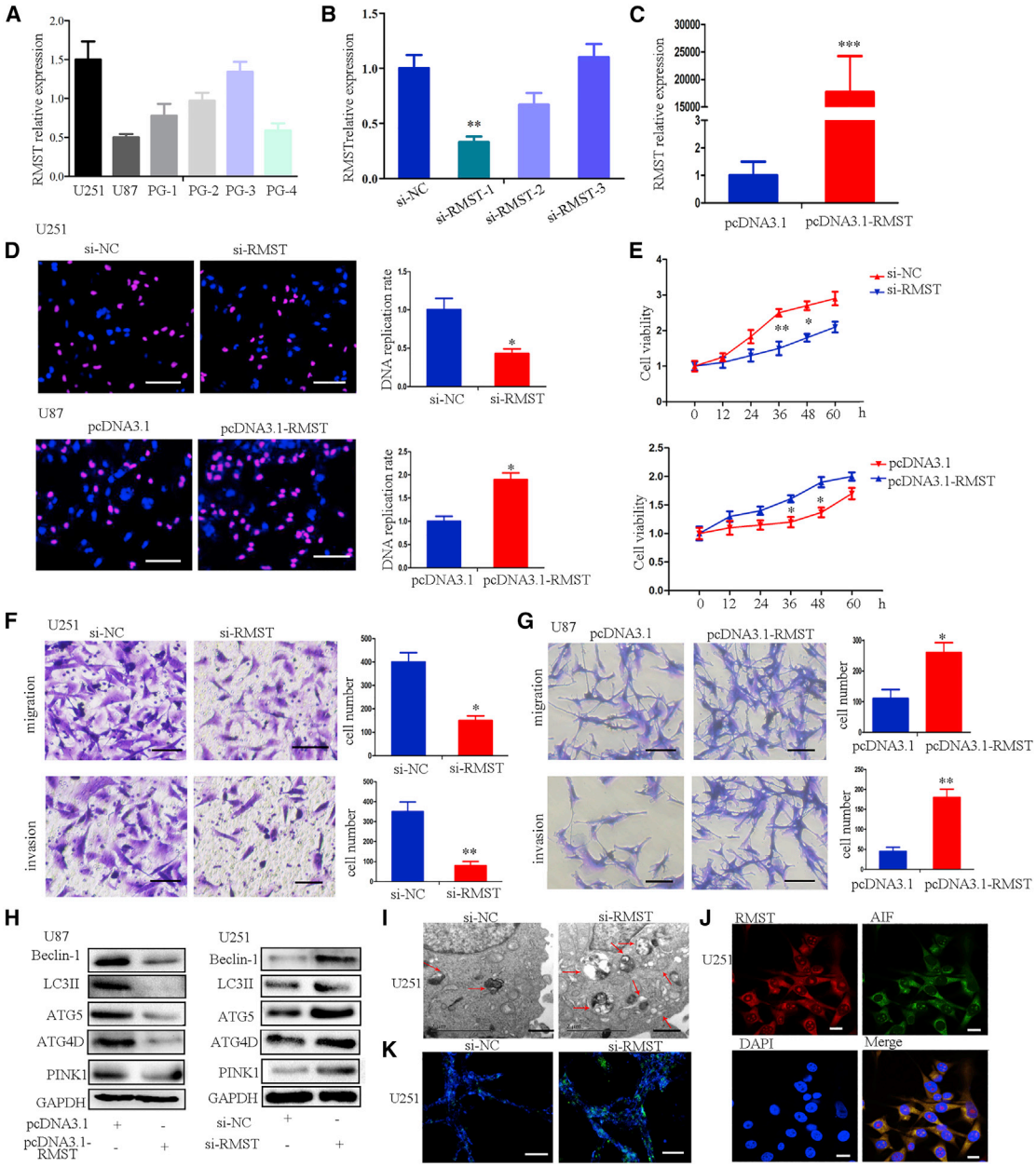

Figure 2. RMST Is a Novel Oncogene and Inhibits GBM Cell Mitophagy

(A) quantitative real-time PCR analysis of RMST expression in astrocytoma cells and primary cultured GBM cells. (B) Knockdown of RMST using three different siRNAs (si-RMST-1, si-RMST-2, and si-RMST-3) or a control siRNA (si-NC) in U251 cells. Data shown are the mean ± SEM of three independent experiments; $^{**}p < 0.01$. (C) Overexpression of RMST in U87 cells. Data shown are the mean ± SEM of three independent experiments; $^{***}p < 0.001$. (D) An EdU assay was performed to assess the proliferation of GBM cells transfected with si-RMST or pcDNA3.1-RMST. The data shown are the means ± SEM of three independent experiments; scale bars, 200 μm. $^{*}p < 0.05$. (E) CCK8 assay was performed to determine the viability of GBM cells transfected with si-RMST or pcDNA3.1-RMST. The data shown are the means ± SEM of three independent experiments. $^{*}p < 0.05$, $^{**}p < 0.01$. (F and G) Transwell assay and Matrigel-coated Transwell assay were performed in U251 and U87 cells that transfected si-RMST or pcDNA3.1-RMST. Data shown are the mean ± SEM of three independent experiments; scale bars, 200 μm; $^{*}p < 0.05$, $^{**}p < 0.01$. (H) Western blotting was performed to detect the level of autophagy markers in GBM cells after knockdown of RMST or overexpression of RMST. (I) Electron microscopy was performed to detect U251 cell autophagy after knockdown of RMST. (J) Representative immunofluorescence staining showing the colocalization of RMST (red) and AIF (green) in U251 cells. Scale bars, 20 μm. (K) Mitophagy staining was performed to detect U251 cell mitophagy after knockdown of RMST. Green, mitophagy dye; scale bars, 200 μm.

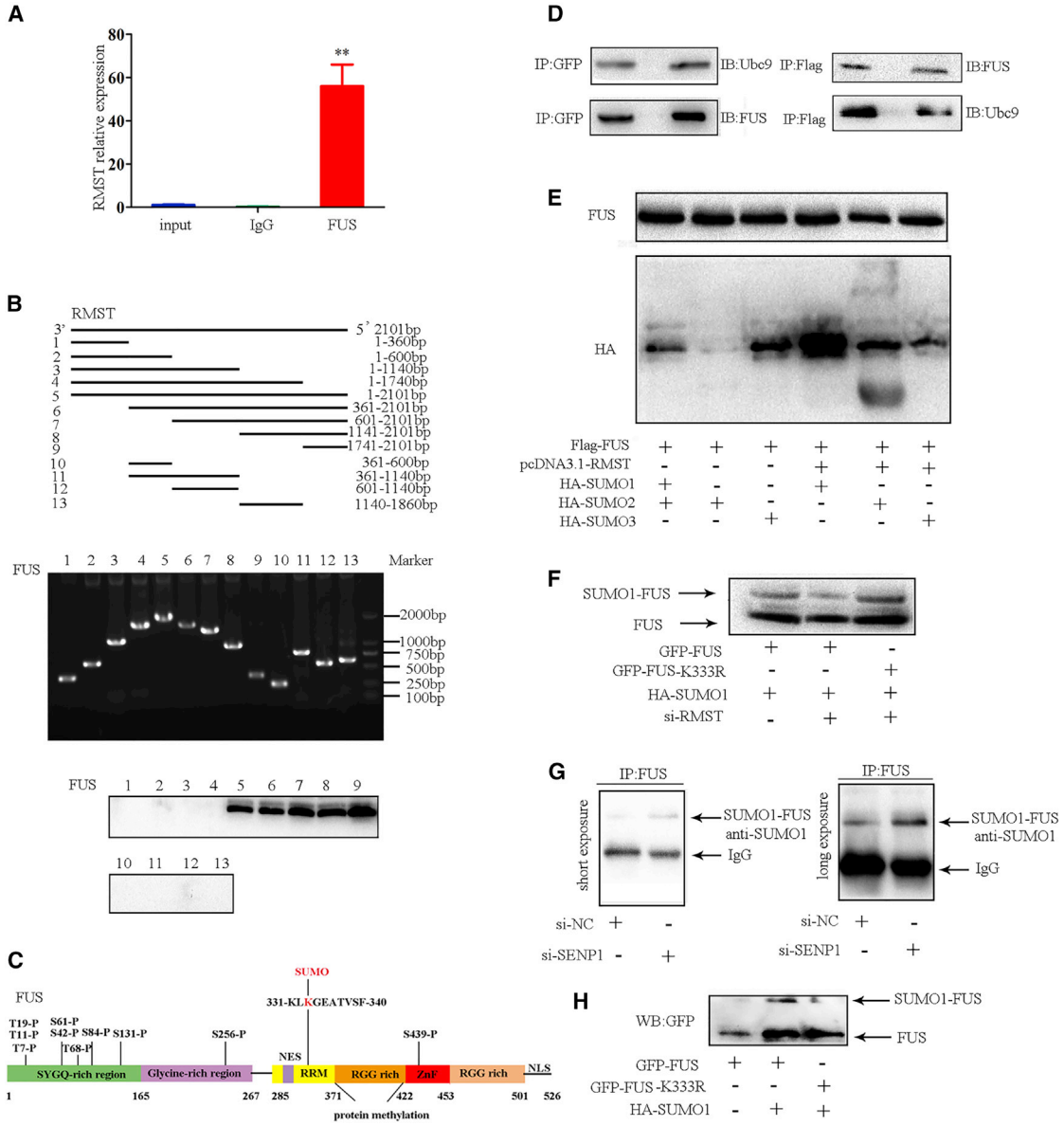

Figure 3. FUS Interaction with RMST and Modified by SUMO1 at K333

(A) RIP-qPCR assay was performed to detect the binding of RMST with FUS in U251 cells. The data shown are the means ± SEM of three independent experiments; *p < 0.05. (B) Upper, schematic illustration of substitution mutant constructs of RMST; middle and lower, an RNA pull-down assay examined the interaction between FUS and the different mutants of RMST. (C) Post-translational modification sites of human FUS protein. Red, conservation of FUS SUMO-modified residues. (D) Coimmunoprecipitation (coIP) analysis showing the interaction between Ubc9 and FUS in U251 cells. (E) Western blotting was performed to detect the modification of FUS by SUMO. U251 cells were cotransfected with RMST, FUS, or HA-SUMO1, -2, or -3. (F) Western blotting was performed to detect the modification of FUS by SUMO1. U251 cells were cotransfected with si-RMST, FUS, and HA- SUMO1. (G) Western blotting was performed to detect the SUMO1 of FUS by knockdown SENP1. (H) Western blotting was performed to confirm the SUMO-modified residues, K333.

confirm these findings, we then checked the half-life of endogenous FUS proteins in U251 cells and found that the half-life of wild-type FUS protein was between 70 and 120 min (Figures 4Ba and 4C), whereas the half-life of FUS protein was less than 70 min after FUS K333 mutant (Figures 4Bb and 4C). When we overexpressed RMST in U251 cells, RMST induced the half-life of the wild-type FUS protein maintain to 100 min (Figures 4Bc and 4C), but RMST barely rescued FUS half-life to longer when FUS K333 mutant (Figures 4Bd and 4C). These results suggested that RMST maintained FUS protein stability by SUMO1 modification at K333.

Table 2. Identification of Candidate SUMO Sites of FUS by SUMOplot™ Analysis Program and SUMOsp 2.0 Software

No.	*Pos.*	*Peptide.*	*Score.1*	*Score.2*
1	K333	RETGKL**K**GEATVSF	0.91	12.125
2	K450	NQCKAP**K**PDGPGGG	0.61	5.204
3	K509	GGFGPG**K**MDSRGEH	0.67	4.324
4	K301-311	VADYFKQ**IGIIK**TNK	/	27.47
5	K426	**K**TGQ	0.54	/
6	K356	QRAGDW**K**CPNPTCE	0.32	/
7	K315	IDWFDG**K**EFSGNPI	0.31	/

We further investigated whether the increased stability of FUS that resulted from its SUMOylation was a result of its ubiquitination inhibition and found that the ubiquitination of wild-type FUS was reduced compared with that of the K333R mutation of FUS, indicating that SUMO1 modification of FUS may inhibit its ubiquitination, resulting in increased the stability for its protein. RMST overexpression also inhibited FUS ubiquitination through its SUMOylation (Figure 4D). The above results indicated that FUS SUMOylation induced by RMST stabilized FUS expression and inhibited its ubiquitination.

FUS SUMOylation by RMST Promotes hnRNPD-Mediated ATG4D Stability to Inhibit GBM Cell Autophagy

FUS could shuttle between the nucleus and cytoplasm,[29] and SUMOylation is known to affect the subcellular localization of substrate protein.[30] Further, we wanted to know whether SUMO1 modification by RMST affected FUS subcellular location. We found that SUMO1 modification of FUS could not affect its subcellular location (Figure 4E). There was no binding autophagy-related protein of FUS, which was a negative result and was not shown. But we found that hnRNPD is a potential FUS-interacting protein (Figure 5A). Immunofluorescence confocal images revealed the colocalization of FUS and hnRNPD in U251 cells (Figure 5B), and we co-transfected with FLAG-tagged hnRNPD and GFP-tagged wild-type FUS or its K333R into HEK293 and U251 cells and found that the band representing hnRNPD was detected in the immunoprecipitation result when the cells were transfected with wild-type FUS. It was not detected when the cells were transfected with the FUS K333R (Figure 5C), indicating that SUMOylation was necessary for FUS interacting with hnRNPD. Furthermore, overexpression of hnRNPD increased the protein level of wild-type FUS but not of its mutant K333R (Figure 5D); simultaneously, overexpression of FUS also increased hnRNPD expression (Figure 5E).

It is well known that hnRNPs have critical roles in regulating alternative splicing,[31] and autophagy related 4D cysteine peptidase (ATG4D) generates two different transcript variants. Whether hnRNPD affected ATG4D alternative splicing is still unclear. We found the alternative splicing of ATG4D was not regulated by hnRNPD (Figure 5F). This suggests that there exist other regulatory mechanisms between hnRNPD and ATG4D. It has been recently reported that heterogeneous nuclear ribonucleoprotein K (hnRNPK) could mediate β-actin stabilization;[32] both hnRNPD and hnRNPK belong to the subfamily of ubiquitously expressed heterogeneous nuclear ribonucleoproteins, and we assessed whether hnRNPD regulated ATG4D stabilization. Ectopic expression or knockdown of hnRNPD decreased or increased the protein levels of ATG4D (Figure 5G), but not transcript levels (Figure 5H). Pre-treatment of U251 with cycloheximide prevented the increased ATG4D levels induced by knockdown expression of hnRNPD (Figure 5I). In addition, incubation of U251 cells with MG132 prevented the degradation of ATG4D protein induced by overexpression of hnRNPD (Figure 5J). These results suggest that hnRNPD regulated ATG4D expression by inhibiting ATG4D protein stabilization in GBM cells. Then, we investigated the roles of SUMOylation FUS in hnRNPD-induced ATG4D, we found that knockdown of hnRNPD resulted in increase of ATG4D, which was abolished by being transfected with the FUS mutant K333R (Figure 5K). Meanwhile, we found that hnRNPD could reduce the stability of ATG4D protein. The half-life of ATG4D protein was shortened from 46 to 17 min by overexpression of RMST, but its half-life was 40 min when FUS mutated. The results suggest that the stability of ATG4D protein regulated by hnRNPD was also affected by SUMOylation FUS (Figures 5L and 5M). These data demonstrated that SUMOylation FUS facilitated the hnRNPD-mediated stability of ATG4D. We further found that FUS SUMO1 modification induced by RMST decreased LC3II, Beclin-1, and PINK1 expression (Figure 5N). The results suggested that RMST inhibited GBM cell mitophagy by inducing SUMO1 modification of FUS.

DISCUSSION

In this study, we first found that lncRNA RMST is highly expressed by TCGA database and clinical glioma samples and functioned as an onco-lncRNA, which promotes glioma cells proliferation, migration, and invasion by inhibiting cell mitophagy. Glioma patients with higher RMST expression have a worse prognosis.

Subsequently, we also first demonstrated that RMST is critical for glioma cell mitophagy through regulating FUS SUMOylation. Since the discovery of SUMO, SUMO has become a widely recognized post-translational modification that targets a myriad of proteins. FUS was first discovered in sarcoma, is also known as an RNA binding protein, and can shuttle between cytoplasm and nucleus.[33] FUS is involved in diverse aspects of RNA metabolism (transcription, RNA splicing, RNA transport, and translation regulation), and it could be modified by multiple post-translational modifications, including phosphorylation and methylation of arginine.[34,35] S42, S256, and S439 of FUS could be phosphorylated by the protein kinase, and multiple arginine sites in the RGG region of FUS served as targets for arginine methyltransferase that could be methylated.[6] To our knowledge, there have only been two reported studies investigating the SUMO2 modification of FUS, Blomster et al.[36] identified 382 SUMO2 targets using a novel method based on SUMO protease treatment, including FUS; Tammsalu et al.[37] also found FUS could be modified by SUMO2. In our study, it is the first report that FUS is modified by SUMO1 and SUMO3 in glioma cells, whereas RMST, as a rhabdomyosarcoma 2-associated transcript, interacts with FUS

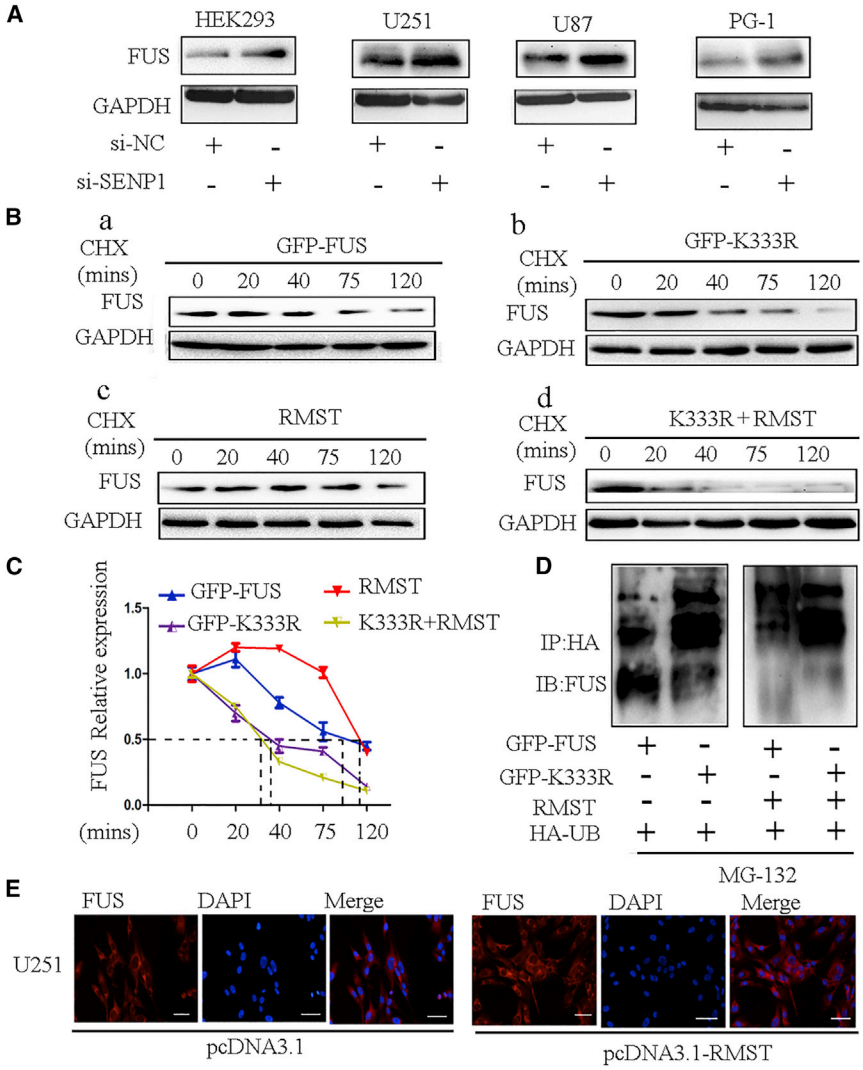

Figure 4. Effect of SUMOylation on the Protein Stability of FUS

(A) Western blotting was performed to detect the expression of FUS in astrocytoma cells after knockdown of SENP1. (B) Western blot was used for measurement of the half-life of FUS after treatment with cycloheximide in U251 cells with GFP-FUS (a), GFP-K333R (b), RMST (c), RMST+K333R (d). (C) Half-life curve for half-life of FUS after treatment with cycloheximide in U251 cells with GFP-FUS, GFP-K333R, RMST, RMST+K333R. (D) Western blot was used to detect the relative amount of ubiquitination FUS in U251 cells; the cells were transfected with GFP-FUS, GFP-K333R, or RMST,GFP-K333R. (E) Representative immunofluorescence staining was used to detect the location of FUS in U251 cells. The cells were transfected with pcDNA3.1-RMST. Scale bars, 50 μm.

and strongly enhances the SUMO1 modification of FUS. We also first identified one lysine residue of FUS that could be modified by SUMO1. Analysis of the amino acids showed that the SUMO consensus motif was [FILMV]Kx[DE].[5] As expected, mutation K333 to arginine (K333R) abolished SUMO1 modification of FUS, probably because this mutation changed the structure of FUS that affects the binding between FUS and SUMO1. Of course, we did not remove other potential SUMO sites; therefore, further studies are needed. Our data reveal that RMST may act as a SUMO enzyme to regulate directly or intensively accelerate the SUMO1 modification of FUS at K333. This was the first report that lncRNA could regulate SUMOylation of protein, and this discovery also enriched the regulation mechanism of lncRNA for post-translational modification.

SUMO exerts a variety of functions. These include changing interaction with DNA, RNA, or proteins, altering enzymatic activities, and modulating other modifications;[38] for example, the crosstalk between SUMO and phosphorylation- and ubiquitin-based signaling are known to us. Our result showed that modification of K333 by SUMO1 affects the function of FUS. The SUMO1 modification of FUS did not affect its localization but contributed to its stability by inhibiting its ubiquitination level; SUMOylation of FUS also affected its interaction with other proteins and stability, such as hnRNPD. hnRNPD is one member of the heterogeneous nuclear ribonucleoprotein family. hnRNPD participates in the regulation of transcription, translation, and mRNA splicing. In this study, we demonstrated that SUMOylation of FUS induced by RMST contributes to the interaction between FUS and hnRNPD. And hnRNPD did not affect the alternative splicing of mitophagy marker ATG4D but maintains and promotes its stability to inhibit mitophagy and tumorigenesis of glioma cells.

Conclusions

Taken together, our results demonstrate a previously unknown function of lncRNA by which RMST binds to FUS and mediates FUS SUMOylation, especially SUMO1 modification at K333. lncRNA RMST suppressed GBM cell mitophagy through enhancing FUS SUMOylation and stabilizing hnRNPD (Figure 6). Our study also indicated that more highly expressed RMST is a prognostic factor for unfavorable outcome of glioma, which will provide a significant guide for the development of medication for gliomas.

MATERIALS AND METHODS

Human Tissue Samples and Cells

Astrocytoma tissues and normal brain tissues were obtained from the Department of Neurosurgery, Xiangya Hospital, Hunan, China.

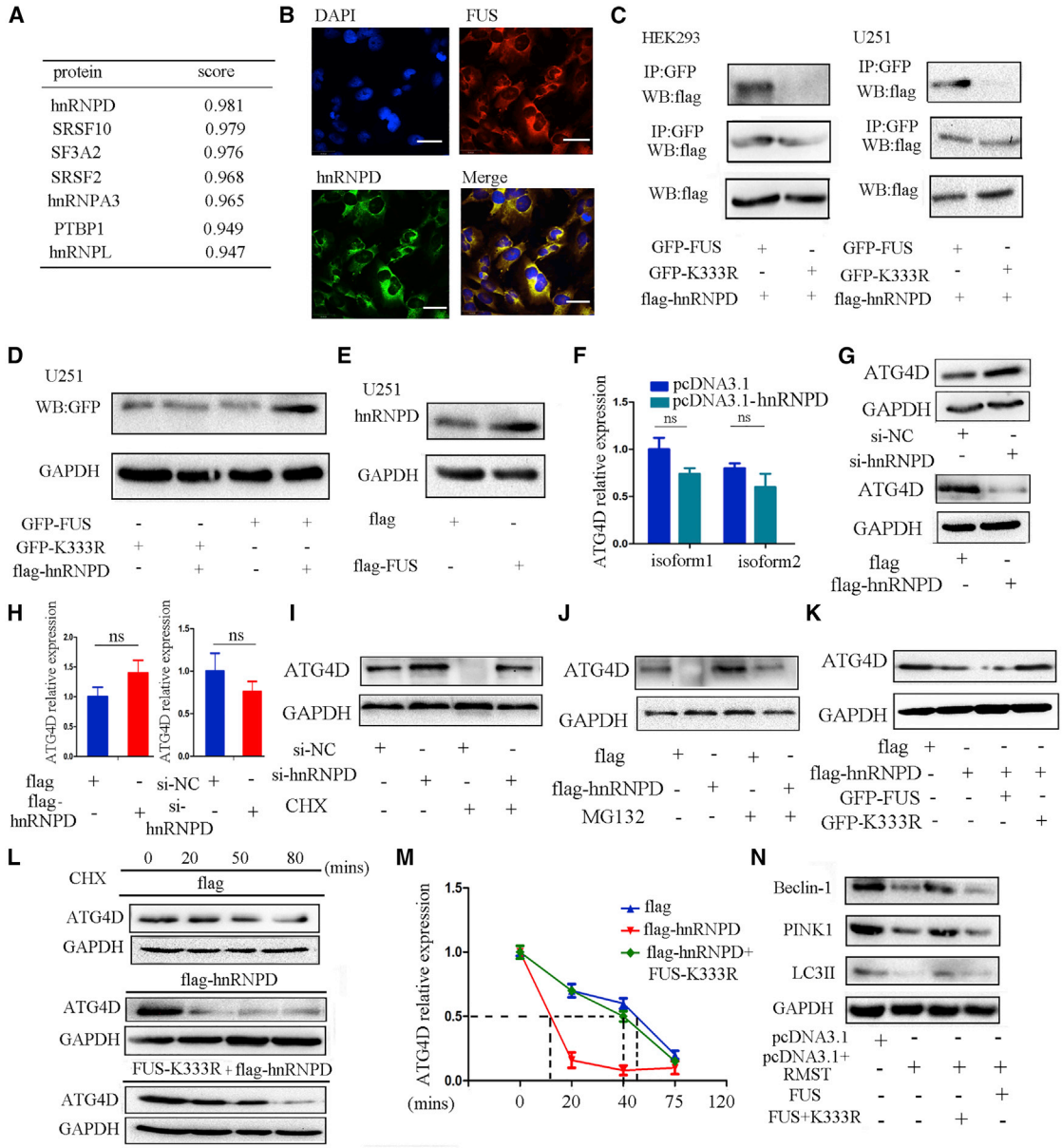

Figure 5. FUS SUMOylation Promotes hnRNPD-Mediated ATG4D Stability to Inhibit GBM Cell Autophagy

(A) Schematic representation potential protein for binding FUS. (B) The colocalization of FUS and hnRNPD was detected by immunofluorescence staining in U251 cells. Scale bar, 29 μm. (C) coIP analysis detected the interaction between FUS and hnRNPD in U251 cells; the cells were cotransfected with GFP-FUS or its mutant K333R with FLAG-hnRNPD. (D) Western blotting was performed to detect the expression of FUS in U251 cells after transfected FUS or its mutant K333R with FLAG-hnRNPD. (E) Western blotting was performed to detect the expression of hnRNPD in U251 cells after overexpression of FUS. (F) quantitative real-time PCR assay was performed to detect the expression of the ATG4D isoform in U251 cells. The cells were transfected with pcDNA3.1-hnRNPD. The data shown are the means ± SEM of three independent experiments. (G) Western blotting was performed to detect the expression of ATG4D in U251 cells after hnRNPD overexpression or knockdown. (H) quantitative real-time PCR was performed to detect the expression of ATG4D in U251 cells after hnRNPD overexpression or knockdown. The data shown are the means ± SEM of three independent experiments. (I) Western blotting analysis was used to measure of the expression of ATG4D after the treatment of U251 cells transfected with or without hnRNPD with cycloheximide. (J) Western blotting analysis detected the expression of ATG4D after the treatment of U251 cells transfected with or without si-hnRNPD with MG132. (K) Western blotting was performed to detect the expression of ATG4D in U251 cells transfected with FUS or its K333 mutant and FLAG-hnRNPD. (L) Western blot analysis to measure the half-life of ATG4D after the treatment of U251 cells transfected with FLAG-hnRNPD or FLAG-hnRNPD and GFP-K333R with cycloheximide. (M) Half-life curve for FUS after the treatment of U251 cells transfected with FLAG-hnRNPD or FLAG-hnRNPD and GFP-K333R with cycloheximide. (N) Western blotting was performed to detect the levels of autophagy markers in GBM cells after cotransfection with GFP-FUS or its K333 mutant and RMST.

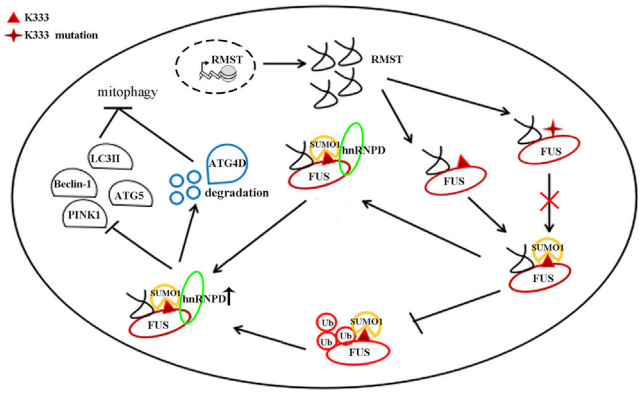

Figure 6. The Model of RMST-Mediated FUS SUMOylation in Regulating GBM Cell Mitophagy

Informed consent was obtained from all patients, and the study was approved by the Ethics Committee of Central South University. U251, U87, and HEK293 cells were from the Cell Center of Peking Union Medical College (Beijing, China). The cells were maintained in DMEM (04-001-1ACS) supplemented with 10% fetal bovine serum (01-052-1ACS). All cells were cultured at 37°C and 5% CO_2. U87 and U251 cell lines were authenticated by short tandem repeat (STR) analysis.

Antibodies and Reagents

The following antibodies were used in this study: FUS (rabbit, Abcam, ab23439, WB1:2000, IP1:200, RIP1:100); LC3B (rabbit, Cell Signaling, 3868, WB1:1000); Beclin-1 (rabbit, Cell Signaling, 3495, WB1:1000); ATG5 (rabbit, Cell Signaling, 12994, WB1:1000); PINK1 (rabbit, Proteintech, 23274-1-AP, WB1:1000); ATG4D (rabbit, Proteintech, 16924-1-AP, WB1:1000); hnRNPD (rabbit, Proteintech, 12770-1AP, WB1:1000); HA (rabbit, Proteintech, 51064-2-AP, WB1:1000); FLAG (mouse, Sigma-Aldrich, F1804, IP1:200); glyceraldehyde-3-phosphate dehydrogenase (GAPDH) (mouse, Proteintech, 60004-1-Ig, WB1:5000); MG132 (Abmole Bioscience, M1902); and cycloheximide (Sigma, R750107).

Immunoprecipitation and Western Blotting Assays

Immunoprecipitation and western blotting assays were performed as previously described. Cells were transfected with specific plasmid or siRNA for 48 h and lysed in an immunoprecipitation (IP) buffer for 30 min. The lysates were centrifuged for 20 min at 12,000 rpm, immunoprecipitated with specific antibodies and IgG, rotated at 4°C for 24 h, and then rotated with protein A/G magnetic beads for 4 h. Immunoprecipitates were washed three times with IP buffer before 4× SDS lysis buffer was added, and then it was analyzed via SDS-PAGE. The proteins were transferred to polyvinylidene difluoride membranes (Merck Millipore, ISEQ00010) and detected with antibodies.

Analysis of SUMO1-Modified FUS

In total, 1×10^7 U251 cells were plated in 10-cm dishes and transfected with 10 μg of FUS, RMST, or HA-SUMO1, HA-SUMO2, or HA-SUMO3. 48 h post-transfection, the cells were lysed in IP buffer. Next, we conducted the IP assay experiments. Rabbit anti-HA was used in IP.

RNA Isolation and quantitative real-time PCR

This procedure was performed as previously described.[19]

The following primers were used:

RMST, 5′-AGCAATGCATTCTTTCACATGG-3′ (forward) and 5′-ATGCAATTTCGGTGGTTGGC-3′ (reverse);

ATG4D, 5′-CCGGACGAAGTGGACAAGTT-3′ (forward) and 5′-GCACTTGCATGACAGCAACA-3′ (reverse); and

GAPDH, 5′-AATGGGCAGCCGTTAGGAAA-3′ (forward) and 5′-GCGCCCAATACGACCAAATC-3′ (reverse).

siRNAs, DNA Plasmids, and Transfection

HA-SUMO1, HA-SUMO2, and HA-SUMO3 were purchased from Addgene, and pcDNA3.1-RMST was purchased from Integrated Biotech Solutions. Cell transfection was performed using Lipofectamine 3000 (Invitrogen-Life Technologies, Carlsbad, CA, USA) according to the manufacturer's instructions. We detected RNA levels after transfecting siRNA and RMST plasmid for 24 h; we detected protein after transfecting HA-SUMO1, HA-SUMO2, HA-SUMO3, and other DNA plasmids for 48 h.

si-NC: 5′-UUCUCCGAACGUGUCACGUTT-3′ (forward) and 5′-ACGUGACACGUUCGGAGAATT-3′ (reverse);

si-RMST: 5′-GGUCGUAUGUCAUUCAAAUTT-3′ (forward) and 5′-AUUUGAAUGACAUACGACCTT-3′ (reverse).

RNA Pull-Down Assay

This procedure was performed as previously described.[23] Biotin-labeled full-length RMST RNA or antisense RMST was heated to 60°C for 10 min, cooled to 4°C, and purified with RNeasy mini kit. Cell extract was mixed with biotin-labeled RNA, washed streptavidin, and agarose beads were added to the reaction. The binding protein was analyzed by western blot assay.

RNA Binding Protein IP

This procedure was performed as previously described.[19] In brief, 5 μg of anti-FUS antibody was used to pull down the RNAs. Then the RNAs were extracted and detected by quantitative real-time PCR.

Mitophagy Detection

U251 cells were plated into 6-well plates and transfected with si-RMST for 48 h. Then, the culture medium was discarded and the cells were washed with D-Hanks. Next, 50 μL 100 nmol/L mitophagy dye working solution was added, followed by incubation at 37°C for 30 min. Afterward, the supernatant was discarded and cells were washed with D-Hanks. Fluorescence microscopy was used to detect the mitophagy.

Transmission Electron Microscopy

U251 cells were transfected with si-RMST for 48 h and fixed with 1% (w/v) OsO_4 in 0.12 M sodium cacodylate buffer for 24 h. The samples were then dehydrated in a graded series of ethanol, transferred to propylene oxide, and embedded in Epon according to standard procedures. Imaging was performed using a Hitachi-7500 transmission electron microscope.

CCK8 Assay, EdU Assay, and Cell Migration and Invasion Assays

These procedures were performed as previously described.[19]

In Situ Hybridization

RMST custom detection probes (Boster, Wuhan, China) were used for *in situ* hybridization. Hybridization, washing, and scanning were performed according to the manufacturer's instructions.

5′-ATACTCTAACTCCGATTATTACCAAAGACAATGTT-3′;

5′-AGATGTGTAGAAATGAACTCTTGTCAGAGTTTCAA-3′;

5′-ATTATTTCTGATGTCTGGAATTTCATTCTCCATGA-3′.

Statistical Analysis

All experiments were analyzed with GraphPad Prism 5 (La Jolla, CA, USA). Differences between the different groups were tested using the Student's t test or one-way ANOVA. The relationships between RMST expression and the clinicopathological parameters were examined using the χ^2 test. overall survival (OS) curves were calculated using the Kaplan-Meier method with the SPSS 15.0 program (SPSS, Chicago, IL, USA). Data are expressed as the mean ± SEM of at least three independent experiments. A probability value of $p < 0.05$ was considered to be statistically significant.

AUTHOR CONTRIBUTIONS

M.W. and C.L. designed the study. C.L., Z.P., P.L., H.F., Y.Z., J.F., T.L., Y.L., and D.L. conducted the experiments. Qing Liu and Qiang Liu acquired and managed patients and provided facilities. M.W. and C.L. wrote the article. M.W. revised of the manuscript. All authors read and approved the final manuscript.

CONFLICTS OF INTEREST

The authors declare no competing interests.

ACKNOWLEDGMENTS

All of the protocols were reviewed and approved by the Ethics Committee of Central South University and performed in accordance with national guidelines. The authors thank PhD Gang Xu and ZeYou Wang for their excellent technical assistance. This work was supported by the National Natural Science Foundation of China (grant number 81874150); the National Key Technology Research and Development Program of the Ministry of Science and Technology of China (grant 2014BAI04B02); the 111 Project (grant number 111-2); and the Graduate Research and Innovation Projects of Central South University (grant number 2017zzts012). Due to our internal policy, raw data cannot be shared.

REFERENCES

1. Li, J., Xu, Y., Long, X.D., Wang, W., Jiao, H.K., Mei, Z., Yin, Q.Q., Ma, L.N., Zhou, A.W., Wang, L.S., et al. (2014). Cbx4 governs HIF-1α to potentiate angiogenesis of hepatocellular carcinoma by its SUMO E3 ligase activity. Cancer Cell *25*, 118–131.

2. Zhao, X. (2018). SUMO-Mediated Regulation of Nuclear Functions and Signaling Processes. Mol. Cell *71*, 409–418.

3. Singh, A.K., Khare, P., Obaid, A., Conlon, K.P., Basrur, V., DePinho, R.A., and Venuprasad, K. (2018). SUMOylation of ROR-γt inhibits IL-17 expression and inflammation via HDAC2. Nat. Commun. *9*, 4515.

4. Gareau, J.R., and Lima, C.D. (2010). The SUMO pathway: emerging mechanisms that shape specificity, conjugation and recognition. Nat. Rev. Mol. Cell Biol. *11*, 861–871.

5. Tatham, M.H., Geoffroy, M.C., Shen, L., Plechanovova, A., Hattersley, N., Jaffray, E.G., Palvimo, J.J., and Hay, R.T. (2008). RNF4 is a poly-SUMO-specific E3 ubiquitin ligase required for arsenic-induced PML degradation. Nat. Cell Biol. *10*, 538–546.

6. Wilson, V.G. (2017). SUMO Regulation of Cellular Processes: Advances in Experimental Medicine and Biology*Second Edition* (Springer).

7. Yu, F., Shi, G., Cheng, S., Chen, J., Wu, S.Y., Wang, Z., Xia, N., Zhai, Y., Wang, Z., Peng, Y., et al. (2018). SUMO suppresses and MYC amplifies transcription globally by regulating CDK9 sumoylation. Cell Res. *28*, 670–685.

8. Bi, H., Li, S., Wang, M., Jia, Z., Chang, A.K., Pang, P., and Wu, H. (2014). SUMOylation of GPS2 protein regulates its transcription-suppressing function. Mol. Biol. Cell *25*, 2499–2508.

9. Song, Y.X., Sun, J.X., Zhao, J.H., Yang, Y.C., Shi, J.X., Wu, Z.H., Chen, X.W., Gao, P., Miao, Z.F., and Wang, Z.N. (2017). Non-coding RNAs participate in the regulatory network of CLDN4 via ceRNA mediated miRNA evasion. Nat. Commun. *8*, 289.

10. Schmitt, A.M., and Chang, H.Y. (2016). Long Noncoding RNAs in Cancer Pathways. Cancer Cell *29*, 452–463.

11. Kopp, F., and Mendell, J.T. (2018). Functional Classification and Experimental Dissection of Long Noncoding RNAs. Cell *172*, 393–407.

12. Chen, L.L. (2016). Linking Long Noncoding RNA Localization and Function. Trends Biochem. Sci. *41*, 761–772.

13. Xing, Z., Lin, A., Li, C., Liang, K., Wang, S., Liu, Y., Park, P.K., Qin, L., Wei, Y., Hawke, D.H., et al. (2014). lncRNA directs cooperative epigenetic regulation downstream of chemokine signals. Cell *159*, 1110–1125.

14. Lin, A., Li, C., Xing, Z., Hu, Q., Liang, K., Han, L., Wang, C., Hawke, D.H., Wang, S., Zhang, Y., et al. (2016). The LINK-A lncRNA activates normoxic HIF1α signalling in triple-negative breast cancer. Nat. Cell Biol. *18*, 213–224.

15. Liu, B., Sun, L., Liu, Q., Gong, C., Yao, Y., Lv, X., Lin, L., Yao, H., Su, F., Li, D., et al. (2015). A cytoplasmic NF-κB interacting long noncoding RNA blocks IκB phosphorylation and suppresses breast cancer metastasis. Cancer Cell *27*, 370–381.

16. Zhang, A., Zhao, J.C., Kim, J., Fong, K.W., Yang, Y.A., Chakravarti, D., Mo, Y.Y., and Yu, J. (2015). LncRNA HOTAIR Enhances the Androgen-Receptor-Mediated Transcriptional Program and Drives Castration-Resistant Prostate Cancer. Cell Rep. *13*, 209–221.

17. Yang, F., Zhang, H., Mei, Y., and Wu, M. (2014). Reciprocal regulation of HIF-1α and lincRNA-p21 modulates the Warburg effect. Mol. Cell *53*, 88–100.

18. Chen, R., Liu, Y., Zhuang, H., Yang, B., Hei, K., Xiao, M., Hou, C., Gao, H., Zhang, X., Jia, C., et al. (2017). Quantitative proteomics reveals that long non-coding RNA MALAT1 interacts with DBC1 to regulate p53 acetylation. Nucleic Acids Res. *45*, 9947–9959.

19. Liu, C., Sun, Y., She, X., Tu, C., Cheng, X., Wang, L., Yu, Z., Li, P., Liu, Q., Yang, H., et al. (2017). CASC2c as an unfavorable prognosis factor interacts with miR-101 to mediate astrocytoma tumorigenesis. Cell Death Dis. *8*, e2639.

20. Xiaoping, L., Zhibin, Y., Wenjuan, L., Zeyou, W., Gang, X., Zhaohui, L., Ying, Z., Minghua, W., and Guiyuan, L. (2013). CPEB1, a histone-modified hypomethylated gene, is regulated by miR-101 and involved in cell senescence in glioma. Cell Death Dis. *4*, e675.

21. Zhang, Y., Feng, J., Fu, H., Liu, C., Yu, Z., Sun, Y., She, X., Li, P., Zhao, C., Liu, Y., et al. (2018). Coagulation Factor X Regulated by CASC2c Recruited Macrophages and Induced M2 Polarization in Glioblastoma Multiforme. Front. Immunol. *9*, 1557.

22. Liu, C., Zhang, Y., She, X., Fan, L., Li, P., Feng, J., Fu, H., Liu, Q., Liu, Q., Zhao, C., et al. (2018). A cytoplasmic long noncoding RNA LINC00470 as a new AKT activator to mediate glioblastoma cell autophagy. J. Hematol. Oncol. *11*, 77.

23. Liu, C., Fu, H., Liu, X., Lei, Q., Zhang, Y., She, X., Liu, Q., Liu, Q., Sun, Y., Li, G., and Wu, M. (2018). LINC00470 Coordinates the Epigenetic Regulation of ELFN2 to Distract GBM Cell Autophagy. Mol. Ther. *26*, 2267–2281.

24. Chan, A.S., Thorner, P.S., Squire, J.A., and Zielenska, M. (2002). Identification of a novel gene NCRMS on chromosome 12q21 with differential expression between rhabdomyosarcoma subtypes. Oncogene *21*, 3029–3037.

25. Yang, F., Liu, Y.H., Dong, S.Y., Yao, Z.H., Lv, L., Ma, R.M., Dai, X.X., Wang, J., Zhang, X.H., and Wang, O.C. (2016). Co-expression networks revealed potential core lncRNAs in the triple-negative breast cancer. Gene *591*, 471–477.

26. Wang, L., Liu, D., Wu, X., Zeng, Y., Li, L., Hou, Y., Li, W., and Liu, Z. (2018). Long non-coding RNA (LncRNA) RMST in triple-negative breast cancer (TNBC): Expression analysis and biological roles research. J. Cell. Physiol. *233*, 6603–6612.

27. Ng, S.Y., Bogu, G.K., Soh, B.S., and Stanton, L.W. (2013). The long noncoding RNA RMST interacts with SOX2 to regulate neurogenesis. Mol. Cell *51*, 349–359.

28. Ng, S.Y., Johnson, R., and Stanton, L.W. (2012). Human long non-coding RNAs promote pluripotency and neuronal differentiation by association with chromatin modifiers and transcription factors. EMBO J. *31*, 522–533.

29. Tan, A.Y., and Manley, J.L. (2012). TLS/FUS: a protein in cancer and ALS. Cell Cycle *11*, 3349–3350.

30. Kim, Y.S., Keyser, S.G., and Schneekloth, J.S., Jr. (2014). Synthesis of 2′,3′,4′-trihydroxyflavone (2-D08), an inhibitor of protein sumoylation. Bioorg. Med. Chem. Lett. *24*, 1094–1097.

31. Geuens, T., Bouhy, D., and Timmerman, V. (2016). The hnRNP family: insights into their role in health and disease. Hum. Genet. *135*, 851–867.

32. Li, D., Wang, X., Mei, H., Fang, E., Ye, L., Song, H., Yang, F., Li, H., Huang, K., Zheng, L., and Tong, Q. (2018). Long Noncoding RNA pancEts-1 Promotes Neuroblastoma Progression through hnRNPK-Mediated β-Catenin Stabilization. Cancer Res. *78*, 1169–1183.

33. De Santis, R., Santini, L., Colantoni, A., Peruzzi, G., de Turris, V., Alfano, V., Bozzoni, I., and Rosa, A. (2017). FUS Mutant Human Motoneurons Display Altered Transcriptome and microRNA Pathways with Implications for ALS Pathogenesis. Stem Cell Reports *9*, 1450–1462.

34. Rhoads, S.N., Monahan, Z.T., Yee, D.S., and Shewmaker, F.P. (2018). The Role of Post-Translational Modifications on Prion-Like Aggregation and Liquid-Phase Separation of FUS. Int. J. Mol. Sci. *19*, E886.

35. Errichelli, L., Dini Modigliani, S., Laneve, P., Colantoni, A., Legnini, I., Capauto, D., Rosa, A., De Santis, R., Scarfò, R., Peruzzi, G., et al. (2017). FUS affects circular RNA expression in murine embryonic stem cell-derived motor neurons. Nat. Commun. *8*, 14741.

36. Blomster, H.A., Hietakangas, V., Wu, J., Kouvonen, P., Hautaniemi, S., and Sistonen, L. (2009). Novel proteomics strategy brings insight into the prevalence of SUMO-2 target sites. Mol. Cell. Proteomics *8*, 1382–1390.

37. Tammsalu, T., Matic, I., Jaffray, E.G., Ibrahim, A.F.M., Tatham, M.H., and Hay, R.T. (2014). Proteome-wide identification of SUMO2 modification sites. Sci. Signal. *7*, rs2.

38. Wilkinson, K.A., and Henley, J.M. (2010). Mechanisms, regulation and consequences of protein SUMOylation. Biochem. J. *428*, 133–145.